Geosci. Model Dev. Discuss., doi:10.5194/gmd-2015-281, 2016
Manuscript under review for journal Geosci. Model Dev.
Published: 20 January 2016

Geoscientific Model Development Discussions
Open Access
EGU

Land surface parameter optimisation through data assimilation: the adJULES system

Nina M. Raoult[1], Tim E. Jupp[1], Peter M. Cox[1], and Catherine M. Luke[1]
[1]National Centre for Earth Observation, University of Exeter, Exeter EX4 4QF, UK
Correspondence to: Nina Raoult (nr278@exeter.ac.uk)

Abstract. Land-surface models (LSMs) are crucial components of the Earth System Models (ESMs) which are used to make coupled climate-carbon cycle projections for the 21st century. The Joint UK Land Environment Simulator (JULES) is the land-surface model used in the climate and weather forecast models of the UK Met Office. In this study, JULES is automatically differentiated using commercial software from FastOpt, resulting in an analytical gradient, or adjoint, of the model. Using this adjoint, the adJULES parameter estimation system has been developed, to search for locally optimum parameter sets by calibrating against observations. This paper describes adJULES and demonstrates its ability to improve the model-data fit using eddy covariance measurements of gross primary production (GPP) and latent heat (LE) fluxes. adJULES also has the ability to calibrate over multiple sites simultaneously. This feature is used to define new optimised parameter values for the 5 Plant Functional Types (PFTS) in JULES. The optimised PFT-specific parameters improve the performance of JULES over 90% of the sites used in the study, a third of which give similar reduction in errors as site specific optimisations. The new improved parameter set for JULES is presented along with the associated uncertainties for each parameter.

1 Introduction

Land-surface models (LSMs) have formed an important component of climate models for many decades now (Pitman, 2003). First generation land-surface schemes focussed on providing the lower boundary condition for atmospheric models by calculating the land-atmosphere fluxes of heat, moisture and momentum, and updating the surface state variables that these fluxes depend on (e.g. soil temperature, soil moisture, snow-cover). In the mid to late 1990s some land-surface modelling groups began to introduce additional aspects of biology into their schemes, most notably the dynamic control of transpiration by leaf stomata and the connected rates of leaf photosynthesis (Sellers et al. (1997); Cox et al. (1999)).

In the early 2000s, climate modelling groups began to use the carbon fluxes simulated by LSMs within first generation climate-carbon cycle models (Cox et al. (2000), Friedlingstein et al. (2001)). These early results, and a subsequent model intercomparison (Friedlingstein et al., 2006), highlighted the uncertainties associated with land carbon-climate feedbacks. The 5th Assessment Report of the Intergovernmental Panel on Climate Change (IPCC AR5 (Stocker et al., 2013)) for the first time routinely included models with an interactive carbon cycle (now called Earth System Models or ESMs), confirming that land responses to climate and CO_2 are amongst the largest of the uncertainties in future climate change projections (Arora and Boer (2005); Brovkin et al. (2013); Jones et al. (2013); Friedlingstein et al. (2013)).

Geosci. Model Dev. Discuss., doi:10.5194/gmd-2015-281, 2016
Manuscript under review for journal Geosci. Model Dev.
Published: 20 January 2016

Geoscientific Model Development Discussions
Open Access
EGU

Uncertainties in LSMs arise from two major sources: (a) process uncertainty, and (b) parameter uncertainty. Process uncertainty includes the misrepresentation of land-surface processes and also the neglect of important processes (such as nitrogen-limitations on plants growth, see for example. Thornton et al. (2007); Zaehle et al. (2010)). The drive to reduce process uncertainty almost invariably leads to increases in LSM complexity, which typically leads to the introduction of additional internal model parameters. Parameter uncertainty arises from uncertainty in these internal model parameters. The evolution of LSMs has therefore involved an attempt to reduce process uncertainty by increasing model realism/complexity, but at the cost of increasing parameter uncertainty. This paper concerns the development and application of a technique to reduce parameter uncertainty in the widely used Joint UK Land Environment Simulator (JULES) LSM (Best et al. (2011); Clark et al. (2011)).

Optimisation techniques come under the umbrella of model-data fusion and range from simple ad-hoc parameter tuning to rigorous data assimilation frameworks. These approaches have been used in a number of studies, covering various LSM, to derive vectors of parameters that improve model-data fit significantly (e.g. Wang et al. (2001, 2007); Reichstein et al. (2003); Knorr and Kattge (2005); Raupach et al. (2005); Santaren et al. (2007); Thum et al. (2008);Williams et al. (2009);Peng et al. (2011)). Many of these studies calibrate the model at individual measurement sites. Given the small spatial footprint of each flux tower, this can often result in over tuning. The optimised model parameters are site-specific and often struggle to perform as well when generalised over other sites(Xiao et al., 2011).

The majority of LSMs group vegetation into a small number of plant functional types (PFTs). Model parameters are assumed to be generic over each PFT. Through different optimisation techniques, some studies have tried to assess the robustness of PFT-specific parameters (e.g. (Kuppel et al., 2014)). Medvigy et al. (2009) and Verbeeck et al. (2011) both show that parameters derived at one site can perform well on a similar site and, in a later study (Medvigy and Moorcroft (2011)), over the surrounding region. However, a contradictory study by Groenendijk et al. (2010) found that there was cross-site parameter variability after optimisation within the PFT groupings.

In the last few years, there has been a move towards deriving PFT-specific parameters using data from multiple sites, the results of which have been generally positive, e.g. Xiao et al. (2011) and Kuppel et al. (2012). Both of these studies used data from multiple sites in their optimisation (calling it multisite optimisation) and have commented on the robustness of this technique showing that the choice of initial parameter vector had little effect on the optimised values.

Kuppel et al. (2012) compared different approaches for finding generic PFT-specific parameters, such as averaging optimised parameter vectors over PFTs and directly optimising over multiple sites. They found that the latter method was best for finding PFT-specific parameters. The multisite optimisation procedure was refined in Kuppel et al. (2014), extended to other PFTs, and evaluated at a global scale.

For global modelling, there is a clear need to find generic parameters and associated uncertainties by PFT, by optimising against observations in a reproducible way. This paper presents a model-data fusion framework that allows data from multiple sites to be used simultaneously in order to improve the JULES land surface model.

This paper aims to answer the following questions:

- Can an optimum vector of generic parameters for each of the JULES PFT classes be found?

Geosci. Model Dev. Discuss., doi:10.5194/gmd-2015-281, 2016
Manuscript under review for journal Geosci. Model Dev.
Published: 20 January 2016

- How does the new PFT parameter vector compare to parameter vectors found by optimising each site individually?
- How robust is the adJULES system when optimising over multiple sites?
- What uncertainty is associated with each parameter?

In section 2, methods and data used in the study are described. The JULES land surface model and our new data assimilation system (adJULES), are described. The data used, and parameters chosen to be optimised in the study, are also discussed. In section 3, the results are presented. The methodology for optimising over multiple sites simultaneously is validated, and optimum parameter values are provided for each JULES PFT. The performance of the new parameter sets is assessed and shown to significantly improve the fit of the JULES model to the observations. The conclusions are laid out in section 4.

2 Methods and Data

2.1 The JULES land-surface model

The JULES land-surface model (Best et al., 2011; Clark et al., 2011) simulates the interactions between the land and atmosphere. Originally developed from the Met Office Surface Exchange Scheme (MOSES) (Cox et al., 1999), JULES can be used 'offline' with observed atmospheric forcing data, or can be coupled into a global circulation model (GCM). JULES is the land surface model used in the UK Met Office Unified Model.

JULES is a mechanistic land surface model including physical, biophysical, and biochemical processes that control the radiation, heat, water, and carbon fluxes in response to time-series of the state of the overlying atmosphere (Best et al., 2011; Clark et al., 2011). Processes such as photosynthesis, evaporation, plant growth and soil microbial activity are all linked through mathematical equations that quantify how soil moisture and temperature govern evapotranspiration, heat balance, respiration, photosynthesis and carbon assimilation (Best et al., 2011; Clark et al., 2011). JULES runs at a given sub-daily step (typically 30 minutes), using meteorological drivers of rainfall, incoming radiation, temperature, humidity and windspeed as inputs.

Vegetation in the JULES model is categorised into five plant functional types (PFTs); broadleaf trees (BT), needleleaf trees (NT), C3 grasses (C3G), C4 grasses (C4G), and shrubs (Sh). Default parameters for these PFT classes are taken from a previous ad hoc calibration (Blyth et al., 2010).

2.2 Data assimilation system

Even a relatively simplistic land-surface representation such as JULES has over a hundred internal parameters representing the environmental sensitivities of the various land-surface types and PFTs within the model. In general these parameters are chosen to represent measurable quantities within the real world (e.g. aerodynamic roughness length, surface albedo, plant root-depth), which allows observationally-based estimates of these parameters to be made in the early stages of the model development process. However, the detailed performance of a land-surface model can be very sensitive to such internal parameters. It is therefore common for land-surface modellers to calibrate their models against available observations (e.g. Blyth et al. (2010)).

Geosci. Model Dev. Discuss., doi:10.5194/gmd-2015-281, 2016
Manuscript under review for journal Geosci. Model Dev.
Published: 20 January 2016

This is typically carried-out in a rather ad hoc manner with the modeller varying the parameters that he/she believes are most relevant to the model performance. Such model tuning is by its very nature subjective, lacks reproducibility, and is often sub-optimal because the modeller is unable to explore the full feasible parameter space through such a manual technique.

This paper describes a more objective approach to land-surface model calibration, adopting ideas from the applied mathematics of data assimilation as used widely in weather forecasting, and motivated by pioneering attempts at carbon cycle data assimilation (Rayner et al. (2005); Kaminski et al. (2013)). It utilises the adjoint of the JULES model (called adJULES), derived by automatic differentiation, which enables efficient and objective calibration against observations. Importantly, adJULES also allows the uncertainties in the best-fit parameters to be estimated. Such uncertainties are important information for model users, and can also form the basis for observation-constrained estimates of prior probability density functions for the land-surface parameter perturbations used in climate model ensembles (e.g. Booth et al. (2012)).

2.2.1 The theory of adJULES

JULES generates a modelled time-series for a given vector of internal parameters, $\boldsymbol{z}$. A cost function, $f(\boldsymbol{z})$ is defined as a weighted sum of squares of differences between the modelled and the observed time-series. The cost consists of the difference between the vector of model outputs at time t, $\boldsymbol{m}_t$ and the vector of observations at time t, $\boldsymbol{o}_t$, combined with a term quadratic in the difference between initial parameter values $\boldsymbol{z}_0$ and values $\boldsymbol{z}$:

$$f(\boldsymbol{z}) = \sum_{t=1}^{s} (\mathbf{m}_t - \mathbf{o}_t)^T \mathbf{R}^{-1} (\mathbf{m}_t - \mathbf{o}_t) + (\boldsymbol{z} - \boldsymbol{z}_0)^T \mathbf{B}^{-1} (\boldsymbol{z} - \boldsymbol{z}_0). \quad (1)$$

Here $\mathbf{R}$ is the observed covariance in the errors $(\mathbf{m}_t - \mathbf{o}_t)$ and $\mathbf{B}$ describes the prior covariances in the parameters with a diagonal matrix proportional to the inverse square of the ranges allowed for each parameter. The constant of proportionality λ, with default value 1, controls the width of the prior distribution and ultimately the relative importance of the background term. Larger values of λ help condition the problem (Bouttier and Courtier, 1999) and force parameter values to be close to the initial value $\boldsymbol{z}_0$. All parameters and observations are equally weighted in this cost function.

The optimal vector of parameters is the vector $\boldsymbol{z}$ that minimises the cost function (Eq. 1). The aim of adJULES is to find this vector. adJULES minimises the cost function iteratively using the gradient descent algorithm L-BFGS-B (Byrd et al. (1995), optim: R Development Core Team (2015)). This algorithm is based on the BFGS quasi-Newton method but is modified to use limited memory and box constraints, so each parameter is given an upper and lower bound based on expert opinion or on physical reasoning (Byrd et al., 1995).

At each iteration, the gradient $\nabla f(\boldsymbol{z})$ of the cost function $f(\boldsymbol{z})$ is computed with respect to all parameters, using the adjoint model of JULES. The adjoint is generated with the automatic differentiator tool TAF (Transformation of Algorithms in Fortran; see Giering et al. (2005)) in 'reverse mode' (rather than 'forward mode') for computational efficiency. Automatic differentiation relies on using the chain rule, the choice of forward or reverse mode refers to the order in which the derivatives are computed. Calculating $\nabla f(\boldsymbol{z})$ is most efficient in reverse mode as only one sweep is needed to generate the derivative with respect to all parameters (Bartholomew-Biggs et al., 2000).

Geosci. Model Dev. Discuss., doi:10.5194/gmd-2015-281, 2016
Manuscript under review for journal Geosci. Model Dev.
Published: 20 January 2016

Geoscientific Model Development Discussions

Once the cost function reaches the minimum, a locally optimal parameter vector z_1 is returned and the second derivative of the cost function with respect to the parameters can be used to calculate posterior uncertainties. This process is then repeated, the locally optimised parameters are fed back through JULES, generating a new modelled time-series and hence a new cost function. The loop is terminates when the modelled time series no longer improves (Fig. 1).

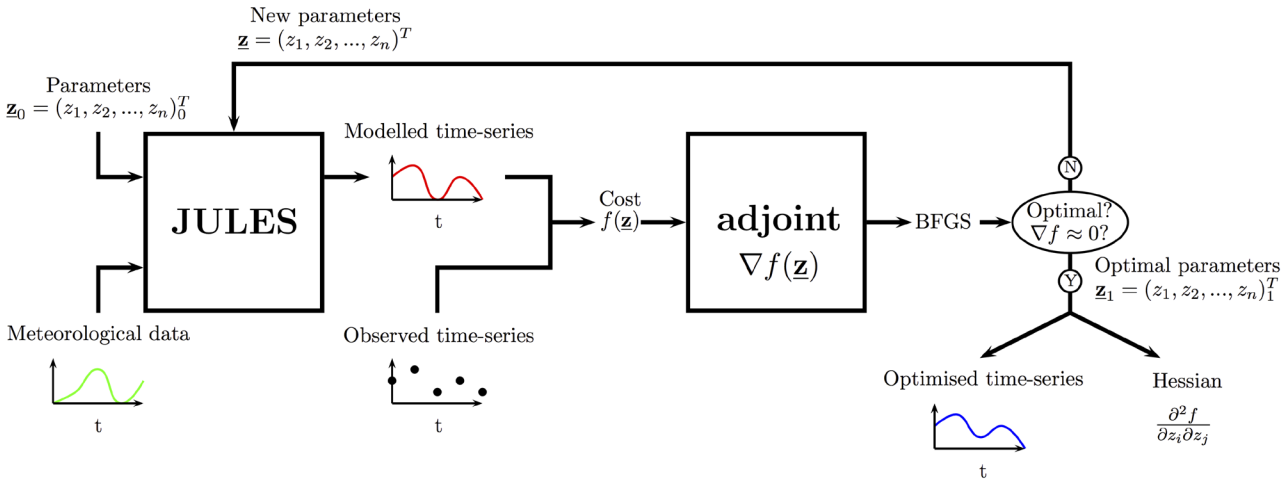

Figure 1. Schematic of the adJULES parameter estimation system starting with the initial parameter vector z_0. This is usually based on default JULES parameter values (Blyth et al., 2010). The optimised parameter vector is denoted z_1.

2.2.2 Multisite Implementation

In its simplest form, adJULES runs at a single grid-point location and so the derived optimal parameter vector is site specific. On the other hand, multisite optimisation aims to find values for a common set of parameters, using data from multiple locations. The definition of the cost function (Eq. 1) can be extended to include the observations from all sites, and its derivative found in order to use the L-BFGS-B algorithm again. The extended cost function is the sum of the individual cost functions for each site. Similarly, the first and second derivatives of this new cost function can be defined using the sum of the derivatives at the individual sites.

2.3 Eddy covariance flux data

The eddy-covariance flux data used in this study are part of the FLUXNET network (Baldocchi et al., 2001). The FLUXNET database contains more than 500 locations worldwide, and all the data is processed in a harmonised manner using the standard methodologies including correction, gap-filling and partitioning (Papale et al., 2006). The sites used in this study were selected based on data availability: sites with missing input variables or significant data gaps during the growing the season were omitted.

Geosci. Model Dev. Discuss., doi:10.5194/gmd-2015-281, 2016
Manuscript under review for journal Geosci. Model Dev.
Published: 20 January 2016

To model photosynthesis Net Ecosystem Exchange (NEE) and Latent Heat Flux (LE), among other fluxes, are required. The NEE flux, defined as the net flux of CO_2, is partitioned into gross primary production (GPP) and ecosystem respiration (Re) (Reichstein et al., 2005). In this study this GPP flux is used, along with the LE flux to constrain the model.

In an attempt to run the experiments as closely to a standard JULES run as possible, input fields of vegetation structure and soil type were drawn from the UK Met Office ancillary files used in the HadGEM2 configurations. The LAI seasonal cycle used is derived from a MODIS product from Boston University. The values taken for each of the experiment sites correspond to the closest grid point with values.

2.4 Experimental setup

Version 2.2 of JULES is implemented in the current version of adJULES. This version is set up to calibrate a subset of JULES soil and vegetation parameters against up to six observables in the vectors $\boldsymbol{m}_t$ and $\boldsymbol{o}_t$ (Eq. 1): net ecosystem exchange (NEE), sensible heat (H), latent heat (LE), surface temperature (T^*), gross primary productivity (GPP) and ecosystem respiration (Resp).

This study aims to improve the parameters used to define PFTs and therefore it concentrates on vegetation parameters. Table 1 outline the parameters chosen.

One year of FLUXNET data is used for each site considered in this study. Where multiple years are available, the most complete year was chosen. For each site, the model is spun up to a steady soil moisture and temperature state. Where possible, the two years of data preceding the year of comparison were repeatedly applied in the spin-up. Where this was not possible, the first year of data was repeatedly applied. Only sites with at least two years of data are used in this study, so that the spin-up year is different from the experiment year. In each case, the model was spun up for at least 50 years. For deciduous sites and crop sites, leaf area index values are taken from MODIS data for the appropriate year.

The sites used in each of the PFT classes are described in Appendix A. The FLUXNET database used in this study did not distinguish between the different types of grasslands. Using Met Office ancillary files, the grasslands were partitioned into C3 grasses and C4 grasses according to fractional cover. In the case of C3 grasses, sites were picked only when the fractional cover was over 60%. Since the C4 grasses are under represented in the FLUXNET database, this boundary was lowered to include all sites where C4 grass was the dominant PFT. Crops were not included in either grass class. The photosynthesis model used in JULES is based on scaling up observed processes at the leaf scale to represent the canopy. The scaling to canopy level can be done in several ways, in this study the simple big leaf approach was adopted (Clark et al., 2011), although optimisations can also be carried-out for more complex canopy radiation options.

All of the sites in each PFT class are used to find the optimal values for the PFT. The second derivative of the cost function found by the adjoint code is then used to quantify the uncertainties associated with these new parameter vectors.

For the multisite experiments, the background term was weighted such that the problem remained conditioned but low enough for useful uncertainties to be generated.

Geosci. Model Dev. Discuss., doi:10.5194/gmd-2015-281, 2016
Manuscript under review for journal Geosci. Model Dev.
Published: 20 January 2016

Geoscientific Model Development Discussions
Open Access
EGU

2.5 Introducing tools for analysis

2.5.1 Different ways to represent parameter uncertainty

As well as generating optimal parameter values, adJULES estimates the uncertainty associated with each parameter. The second derivative (Hessian) of the cost function,

$$H_{ij} = \frac{\partial^2 f}{\partial z_i \partial z_j} \tag{2}$$

where $f(\boldsymbol{z})$ is given by equation (1), evaluated at the optimal parameter value, yields information about the curvature of the cost function at the local minimum. A 'sharp' cost function, where the cost function is steep either side of the optimal parameter value indicates lower parameter uncertainty. This can also be interpreted as meaning that a small deviation from the optimal parameter value yields a large increase in cost. Conversely, a 'flat' cost function indicates higher parameter uncertainty, or little change in cost caused by deviation from the optimal parameter value.

In order to generate statistics associated with the curvature of the cost function, the Hessian is used to generate a truncated multivariate normal distribution (Genz et al., 2015). Using Gibbs sampling (Geman and Geman, 1984), an ensemble of plausible parameter vectors is generated from this distribution, for a statistically satisfactory match between observations and modelled time series. The multivariate normal parameter distribution allows for marginal density plots to be generated for each parameter. When considering these marginal density plots, it is important to remember that they represent only one or two dimension of an n-dimensional multivariate normal distributions. The optimal parameter values may not correspond to the peak of the one-dimensional distributions as a result.

2.5.2 Metric to quantify model fit to data

To measure the improvement exhibited by different parameter vectors, a normalised root-mean-square deviation (ϵ) is used.

Given a parameter vector, $\boldsymbol{z}$, a modelled time series $\boldsymbol{m}_{i,t}$ with k data points is generated using JULES, where i denotes one of the LE and GPP data streams. For each data stream i, the ϵ normalised error is calculated as follows

$$\epsilon_i = \sqrt{\frac{\sum_{t=1}^{k}(\boldsymbol{m}_{i,t} - \boldsymbol{o}_{i,t})^2}{k}}, \tag{3}$$

and then normalised:

$$\hat{\epsilon}_i = \frac{\epsilon_i}{\max(\boldsymbol{m}_{i,t}, \boldsymbol{o}_{i,t}) - \min(\boldsymbol{m}_{i,t}, \boldsymbol{o}_{i,t})}. \tag{4}$$

After non-dimensionalising both data streams, the final error is given by

$$\hat{\epsilon} = \frac{\hat{\epsilon}_1 + \hat{\epsilon}_2}{\sqrt{2}}. \tag{5}$$

This ensures values are between 0 and 1; 0 representing a perfect match to the observations, 1 a complete mismatch. The closer the value is to 0, the better the set of parameters $\boldsymbol{z}$ used is at creating modelled time-series resembling the observed time-series.

Geosci. Model Dev. Discuss., doi:10.5194/gmd-2015-281, 2016
Manuscript under review for journal Geosci. Model Dev.
Published: 20 January 2016

3 Results and discussion

In this section, the site-specific optimisations are first considered. By considering each PFT separately, the misfits between the model and the observations are discussed and the effect of optimising over each site individually to improve model-observation agreement is considered.

Next, the multisite methodology is validated. This is then used to perform optimisations over each of the PFTs. All of the sites in a given PFT are optimised simultaneously to find a generic parameter vector appropriate to the PFT. The new optimised parameter vectors are presented, along with associated uncertainties. The rest of the section considers the improvement found using these optimised parameter vectors, and discusses some of the uncertainties and correlations found.

3.1 Single-site optimisations

First, each of the sites was optimised individually in order to find site-specific parameter vectors. As described in section 2.4, one year runs at the different sites were optimised against monthly averaged LE and GPP. A site dominated by each PFT was picked to represent the general improvements made. The main seasonal cycles of latent heat and GPP for the different sites are shown in Fig. 2.

Most broadleaf sites follow the pattern of Fig. 2(a). Normally, for broadleaf sites, a standard JULES run will underestimate GPP. The optimisation does a good job in fixing this, bring the modelled time-series closer to the observations. In contrast, LE does not improve as much.

Similarly for the needleleaf sites (Fig. 2(b)), the JULES model output tends to overestimate LE and underestimate GPP. The parameter vector found in the optimisation improves the fit of both data streams, most notably GPP. At sites for which a double peak seasonality is apparent, the optimised model captures this better than the original model.

GPP is also underestimated for the C3 grass sites (Fig. 2(c)) and, for the majority of the sites, the optimisation does a good job of correcting this. The LE flux tends to be at the right magnitude before optimisation, unlike the GPP flux, but adJULES does not manage to improve this output significantly. In the example shown, the JULES model using the default parameter already performs very well, so little improvement is needed, but this is not always the case. The new set of parameters is also good at simulating multiple peaks in the LE and GPP fluxes, when they are observed.

There are only two C4 grass sites in the set and JULES does not perform very well on these before or after optimisation (Fig. 2(e)).

The shrub sites, Fig. 2(f), show no general pattern. Some sites overestimate LE, whilst others underestimated it, and similarly for GPP. The levels of improvement varies over sites. For some of the sites in this PFT, the magnitude of GPP fails to get close to the magnitude of the observations, both before and after optimisation. However, it is hard to pick out a general pattern for this PFT, since there are only 5 sites in this set.

Overall, the adjoint performs well in improving the performance of JULES at individual sites, regardless of PFT. The systematic underestimation of GPP in default JULES, improves the most. This larger improvement in GPP fit reflects the larger

Geosci. Model Dev. Discuss., doi:10.5194/gmd-2015-281, 2016
Manuscript under review for journal Geosci. Model Dev.
Published: 20 January 2016

Geoscientific Model Development Discussions
Open Access
EGU

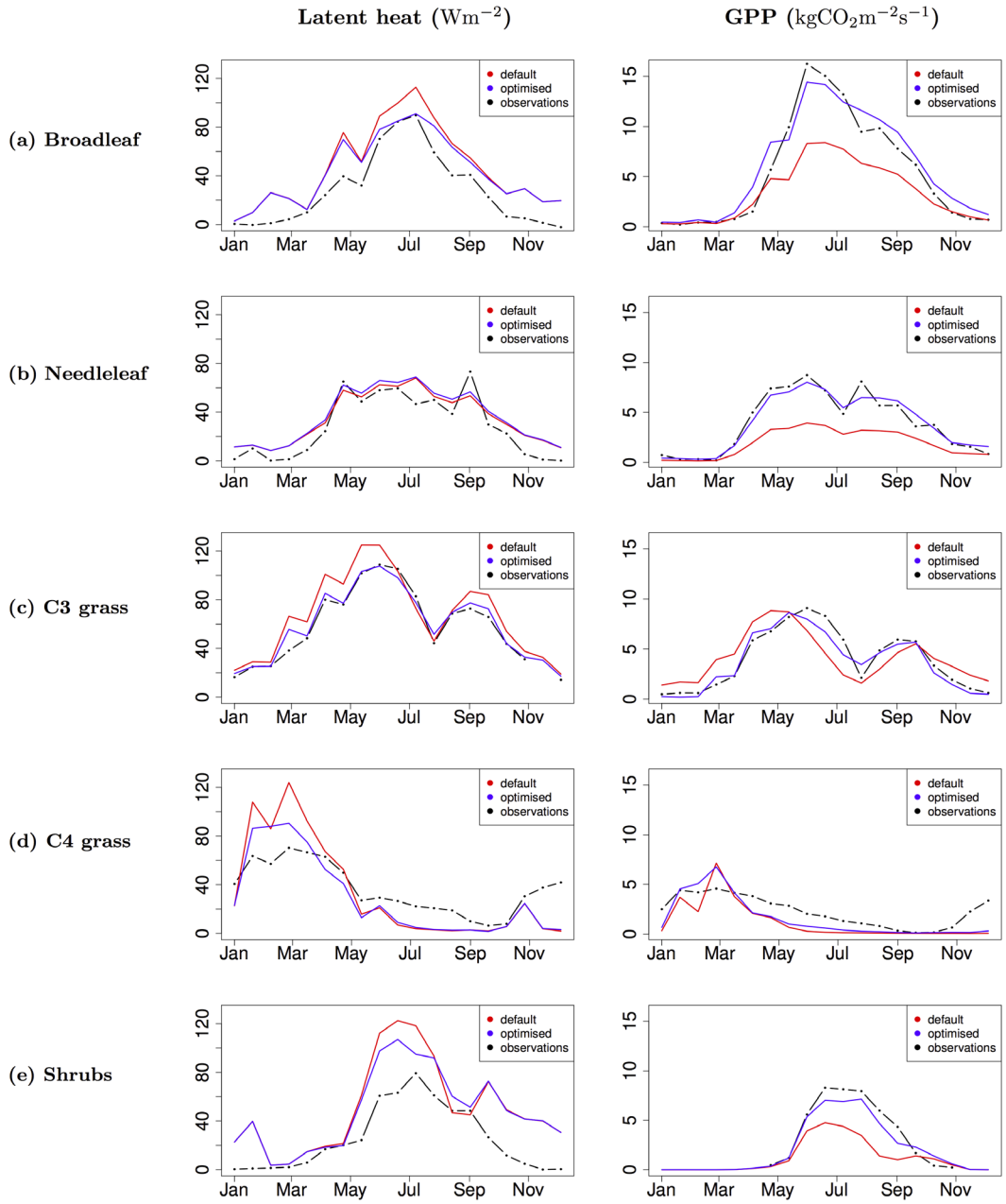

Figure 2. Time-series plots for LE (left) and GPP (right) for a single site in each of the different PFTs. Observations (black) are compared to the original JULES runs (red) and the runs using the optimal parameters found at each individual site locally (blue).

set of optimised parameters that are exclusively related to the carbon cycle. Different parameters may need to be incorporated, for example some soil ones, for the LE flux to improve further.

Geosci. Model Dev. Discuss., doi:10.5194/gmd-2015-281, 2016
Manuscript under review for journal Geosci. Model Dev.
Published: 20 January 2016

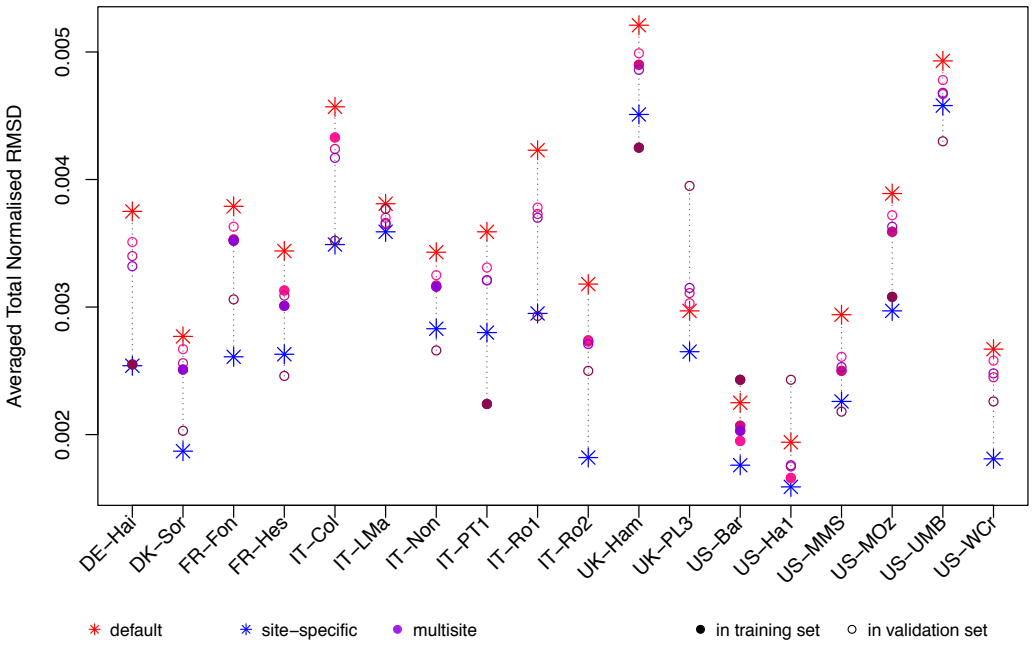

Figure 3. The effect of parameter vectors z vectors on the overall model-data fit at each of the sites tested, using the metric described in section 2.5.2. Original default JULES parameters (∗), site-specific optimal parameters (∗), and the multisite parameters found by optimising over each set of five sites (●○,●○,●○,●○), denoted set 1, set 2, set 3, set 4 respectively. Sites in the training set (filled circles), sites in validation set (open circles).

3.2 Multisite Validation

Broadleaf sites were used to validate the multisite methodology. This PFT is the best represented in the FLUXNET network, though since the broadleaf set is large and spans a wide range of climatologies, only deciduous sites were considered.

Optimisation was performed four randomly selected sets of five sites were. The optimal parameter vectors were then tested at the remaining sites. The results are shown in Fig. 3.

The optimised parameter vectors generally perform well, both on the sites used in the training sets and the sites used in the validations sets. Indeed 15/18 of the sites improve no matter which of the optimised parameter vectors are used. The parameter vector optimised over set 3 performs even better than the individual optimisations for some of the sites. JULES performed worse on just two sites (UK-PL3, US-Ha1) using these parameter values compared to the default JULES parameters. These two sites also start off with relatively small errors, so even with the slight increase in errors they are still among the best performing sites in the set. UK-PL3 does not improve with any of the 5-site parameter sets, but observations from this site appears to be somewhat unusual (e.g. it has a very different seasonality to the rest of the sites for this PFT).

Geosci. Model Dev. Discuss., doi:10.5194/gmd-2015-281, 2016
Manuscript under review for journal Geosci. Model Dev.
Published: 20 January 2016

It seems likely that the adding more sites to a multisite optimisation smooths the cost function and makes it less likely for the optimisation to get stuck in local minima. This may be one of the reasons that some of the 5-site optimisation works better than the single-site optimisation for certain sites.

Overall the results are promising, showing that the optimised parameters, even when calibrated from a small subset of sites, can be generalised over the rest of the set.

3.3 New PFT parameter values

Optimisations were performed over all available sites for each of the PFTs simultaneously. The optimised model parameters for each of the PFTs are presented in Fig. 4.

For half of the parameters, the original parameter value is found outside the new uncertainty bounds. The $\frac{\delta c}{\delta l}$ parameter, which determines the efficiency of rainfall interception by the plant canopy, does not change much from its original value for any of the PFTs. The uncertainty bounds are relatively tight and symmetrical. The rest of the parameters show more variation. As described in section 2.5.1, the optimal values need not be in the centre of the uncertainty range, the uncertainties can be skewed. Most the PFTs display high uncertainty in at least one of the the parameters optimised; for the optimised broadleaf set for example, dq_c is highly unconstrained. For C4 grasses, d_r is so unconstrained, even the optimal value found is outside of the 80% confidence interval. C3 grasses shows large uncertainty in n_0 and for shrubs, the parameter with the largest uncertainty is α.

The uncertainties shown in Fig. 4 are one-dimensional marginal distributions. To understand further how the parameters are correlated, consider the two-dimensional representation in Fig. 5. For all the PFTs, the new parameter uncertainties exclude a large part of the prior ranges.The cloud of plausible points tends to be restrictive and tight for most parameters.

The majority of the broadleaf parameters, shown in Fig. 5(a), are highly correlated with each other. The d_r and $\frac{\delta c}{\delta l}$ parameters are the only ones to be uncorrelated with other parameters. Similarly, the needleleaf parameters (Fig. 5(b)) are all highly correlated, either positively or negatively, except for T_{low}, which is completely uncorrelated with any of the other parameters.

For C3 grasses,(Fig. 5(c)), the parameters which show no correlation between themselves and any other parameters are T_{low} and $\frac{\delta c}{\delta l}$. The d_r parameters shows varying levels of correlations with the other parameters. The rest of the parameters are highly correlated.

All the C4 grass parameters (Fig. 5(d)) are completely uncorrelated, with the exception of of the parameter pair d_r and dq_c, which covary. For the shrub optimised parameters (Fig. 5(e)) , n_0 is negatively correlated with f_0 and dq_c. The rest of the parameters are not correlated.

The parameter vectors showing the highest correlations belong to the broadleaf and the needleleaf optimisations, for which there are more measurement sites. Such a high correlation between parameters may therefore be related to the number of sites used in the optimisation.

Geosci. Model Dev. Discuss., doi:10.5194/gmd-2015-281, 2016
Manuscript under review for journal Geosci. Model Dev.
Published: 20 January 2016

3.3.1 The performance of the new PFT parameters

The performance of the PFT-specific parameters are compared to the default JULES values and the results of the model optimised independently at each measurement site. This is shown in Fig. 6. The lower the error, the better the model fits the observations, and so the better performing the parameter vector is.

All sites are improved using the locally optimised parameter vectors. For the majority of sites, this decrease in error is substantial. Only the outliers, which start with large initial errors, and the C4 grass site show little improvement. For the C4 grass sites, the initial error is low due to the fact these sites have incomplete data.

The new PFT-specific parameter vectors improve JULES performance over 92% of the sites used in this study. The new broadleaf parameter vector significantly improves 25 of the 28 broadleaf sites, and a further two of the sites give errors similar to when the default parameters are used. Only UK-PL3 gets notably worse. Considering this site more closely, it can be seen to behave differently from the rest of the sites in the set, both in magnitude of the fluxes and seasonality.

The needleleaf sites improve greatly when using the new needleleaf parameter values, with a third of the sites nearly performing as well as the single-site optimisations. The only site this new parameter vector does not improve is CA-Qcu, which was one of the sites with the lowest initial error. As with averaging, sites with the best fit may have to be sacrificed to achieve a generic parameter set across the PFT. The new error still remains relatively low.

For the C3 grass site, there is a reduction in error for 9 of the 11 sites when using the new parameters. The last two sites in the set act similarly to when the default parameters were used. For the C4 grass sites, which started with relatively low errors, the new parameter vector improves the sites slightly. However, the set of two sites is too small to draw any proper conclusion about the C4 grass parameters. There is a clear need for more data from C4 grass sites. Finally, the Shrubs can be seen to improve for all the sites.

In the case of the outliers, the new PFT-specific parameter vectors improves JULES performance even relative to the single-site optimisations. A further 9 sites of the whole set of sites improve to a greater extend than the local optimisations.

4 Conclusions

adJULES enables objective calibration of JULES against observational data, providing best fit internal parameters and the associated uncertainty ranges. The adJULES fits of JULES against individual FLUXNET sites show significant improvements in the performance of JULES compared to default parameters, typically in both the simulation of LE and GPP. All of the sites in this study improve when optimised locally, with the GPP flux improving most significantly.

The study is partially motivated by the desire to improve the performance of JULES within the Hadley Centre's Earth System Models, which means needing to find best fit parameters for a relatively small number of PFTs. This is achieved by classifying the FLUXNET sites into groups dominated by each JULES PFT (BT, NT, C3G, C4G, Sh) and using adJULES to find the best fit parameters for each of these PFT groupings. Although the PFT-specific parameters inevitably do not fit the data as well as site-specific parameters, they still offer significant improvements of the default JULES parameters. For over 90% of the sites, the new PFT-specific parameters are better than default parameters giving closer model-data fit.

Geosci. Model Dev. Discuss., doi:10.5194/gmd-2015-281, 2016
Manuscript under review for journal Geosci. Model Dev.
Published: 20 January 2016

For some PFTs (notably C4G and Shrubs) there are insufficient FLUXNET sites to determine optimal parameters satisfactorily. Additional data and sites for these PFTs are therefore urgently required.

It is, however, clear that there are some limitations to the success of the optimisation results. Certain sites still show significant differences between model output and observations. These issues indicate that improvement to model physics may be necessary in order to produce better model output. This is because adJULES produces the best possible fit to observations, given the existing model physics and the prescribed driving data. If the fit is still inadequate, it is down to the model and data themselves, rather than parameter values. adJULES therefore also enables model structural errors to be identified.

A successful and robust multisite optimisation assumes that sites can be grouped and parameter values can apply to several sites at once. Whilst the PFT generic parameters show great improvement, agreeing with the general 5-PFTs definition found in JULES, there is a possibility to rethink the PFT definitions and group sites differently. This could be done either by looking more closely at the site specifics detailed by the FLUXNET database, or by considering the single-site optimisations and performing a cluster analysis to empirically identify PFTs.

Code availability

The source code of the adJULES data assimilation system is available at http://adjules.ex.ac.uk/. JULES land surface model is freely available to any researcher for non-commercial use. Version 2.2 used in this study can be requested at jules.jchmr.org. The main documentation for the JULES system can also be found at this site. The adjoint of the JULES model has been generated using commercial software TAF (sect. 2.2.1). For licensing reasons, the recalculation of the adjoint following code changes can only be done by us here at Exeter.

Geosci. Model Dev. Discuss., doi:10.5194/gmd-2015-281, 2016
Manuscript under review for journal Geosci. Model Dev.
Published: 20 January 2016

Geoscientific Model Development Discussions

Appendix A

Appendix B

Acknowledgements. This work was supported by the UK Natural Environment Research Council (NERC) through the National Centre for Earth Observation (NCEO).

This study used eddy-covariance data acquired by the FLUXNET community and in particular by the following networks: AmeriFlux (U.S. Department of Energy, Biological and Environmental Research, Terrestrial Carbon Program (DE-FG02-04ER63917 and DE-FG02-04ER63911)), AfriFlux, AsiaFlux, CarboAfrica, CarboEuropeIP, CarboItaly, CarboMont, ChinaFlux, Fluxnet-Canada (supported by CFCAS, NSERC, BIOCAP, Environment Canada, and NRCan), GreenGrass, KoFlux, LBA, NECC, OzFlux, TCOS-Siberia, USCCC.

Further acknowledgements goes to the financial support to the eddy covariance data harmonisation provided by CarboEuropeIP, FAO-GTOS-TCO, iLEAPS, Max Planck Institute for Biogeochemistry, National Science Foundation, University of Tuscia, Université Laval and Environment Canada and US Department of Energy and the database development and technical support from Berkeley Water Center, Lawrence Berkeley National Laboratory, Microsoft Research eScience, Oak Ridge National Laboratory, University of California - Berkeley, University of Virginia.

Thanks to T. Kaminski and R.Giering from FastOpt for their contribution to the development of the adjoint model. Finally, thanks to M.Groenendijk, A.Harper, and the UK Met Office for processing and sharing their data.

Geosci. Model Dev. Discuss., doi:10.5194/gmd-2015-281, 2016
Manuscript under review for journal Geosci. Model Dev.
Published: 20 January 2016

References

Arora, V. and Boer, G.: A parameterization of leaf phenology for the terrestrial ecosystem component of climate models, Global Change Biology, 11, 39–59, 2005.

Baldocchi, D., Falge, E., Gu, L., Olson, R., Hollinger, D., Running, S., Anthoni, P., Bernhofer, C., Davis, K., Evans, R., et al.: FLUXNET: a new tool to study the temporal and spatial variability of ecosystem-scale carbon dioxide, water vapor, and energy flux densities, Bulletin of the American Meteorological Society, 82, 2415–2434, 2001.

Bartholomew-Biggs, M., Brown, S., Christianson, B., and Dixon, L.: Automatic differentiation of algorithms, Journal of Computational and Applied Mathematics, 124, 171 – 190, doi:http://dx.doi.org/10.1016/S0377-0427(00)00422-2, http://www.sciencedirect.com/science/article/pii/S0377042700004222, numerical Analysis 2000. Vol. IV: Optimization and Nonlinear Equations, 2000.

Best, M. J., Pryor, M., Clark, D. B., Rooney, G. G., Essery, R. L. H., Ménard, C. B., Edwards, J. M., Hendry, M. A., Porson, A., Gedney, N., Mercado, L. M., Sitch, S., Blyth, E., Boucher, O., Cox, P. M., Grimmond, C. S. B., and Harding, R. J.: The Joint UK Land Environment Simulator (JULES), Model description - Part 1: Energy and water fluxes, Geoscientific Model Development Discussions, 4, 595–640, doi:10.5194/gmdd-4-595-2011, 2011.

Blyth, E., Lloyd, A., Gash, J., Pryor, M., Weedon, G., and Shuttleworth, J.: Evaluating the JULES Land Surface Model Energy Fluxes Using FLUXNET Data, Journal of Hydrometeorology, 2010.

Booth, B. B. B., Dunstone, N. J., Halloran, P. R., Andrews, T., and Bellouin, N.: Aerosols implicated as a prime driver of twentieth-century North Atlantic climate variability, Nature, 484, 228–232, http://dx.doi.org/10.1038/nature10946, 2012.

Bouttier, F. and Courtier, P.: Data assimilation concepts and methods, Training, pp. 1–59, 1999.

Brovkin, V., Boysen, L., Raddatz, T., Gayler, V., Loew, A., and Claussen, M.: Evaluation of vegetation cover and land-surface albedo in MPI-ESM CMIP5 simulations, Journal of Advances in Modeling Earth Systems, 5, 48–57, doi:10.1029/2012MS000169, http://dx.doi.org/10.1029/2012MS000169, 2013.

Byrd, R., Lu, P., Nocedal, J., and Zhu, C.: A limited memory algorithm for bound constrained optimization, SIAM Journal on Scientific Computing, 16, 1190–1208, 1995.

Clark, D. B., Mercado, L. M., Sitch, S., Jones, C. D., Gedney, N., Best, M. J., Pryor, M., Rooney, G. G., Essery, R. L. H., Blyth, E., Boucher, O., Harding, R. J., and Cox, P. M.: The Joint UK Land Environment Simulator (JULES), Model description - Part 2: Carbon fluxes and vegetation, Geoscientific Model Development Discussions, 4, 641–688, doi:10.5194/gmdd-4-641-2011, http://www.geosci-model-dev-discuss.net/4/641/2011/, 2011.

Cox, P., Betts, R., Jones, C., Spall, S., and Totterdell, I.: Acceleration of global warming due to carbon-cycle feedbacks in a coupled climate model, Nature, 408, 184–187, 2000.

Cox, P. M., Betts, R. A., Bunton, C. B., Essery, R. L. H., Rowntree, P. R., and Smith, J.: The impact of new land surface physics on the GCM simulation of climate and climate sensitivity, Climate Dynamics, 15, 183–203, 1999.

Friedlingstein, P., Bopp, L., Ciais, P., Dufresne, J.-L., Fairhead, L., LeTreut, H., Monfray, P., and Orr, J.: Positive feedback between future climate change and the carbon cycle, Geophysical Research Letters, 28, 1543–1546, doi:10.1029/2000GL012015, http://dx.doi.org/10.1029/2000GL012015, 2001.

Friedlingstein, P., Bopp, L., Rayner, P., Cox, P. M., Betts, R., Jones, C., Von Bloh, W., Brovkin, V., Cadule, P., Doney, S., et al.: Climate–carbon cycle feedback analysis: results from the C4MIP model intercomparison, Journal of Climate, 19, 3337–3353, 2006.

Geosci. Model Dev. Discuss., doi:10.5194/gmd-2015-281, 2016
Manuscript under review for journal Geosci. Model Dev.
Published: 20 January 2016

Friedlingstein, P., Meinshausen, M., Arora, V. K., Jones, C. D., Anav, A., Liddicoat, S. K., and Knutti, R.: Uncertainties in CMIP5 Climate Projections due to Carbon Cycle Feedbacks, Journal of Climate, 27, 511–526, doi:10.1175/JCLI-D-12-00579.1, http://dx.doi.org/10.1175/JCLI-D-12-00579.1, 2013.

Geman, S. and Geman, D.: Pattern Analysis and Machine Intelligence, IEEE Transactions on, Stochastic Relaxation, Gibbs Distributions, and the Bayesian Restoration of Images, 1984.

Genz, A., Bretz, F., Miwa, T., Mi, X., Leisch, F., Scheipl, F., and Hothorn, T.: mvtnorm: Multivariate Normal and t Distributions, 2015.

Giering, R., Kaminski, T., and Slawig, T.: Generating efficient derivative code with TAF: Adjoint and tangent linear Euler flow around an airfoil, Future Generation Computer Systems, 21, 1345 – 1355, doi:http://dx.doi.org/10.1016/j.future.2004.11.003, http://www.sciencedirect.com/science/article/pii/S0167739X04001785, 2005.

Groenendijk, M., Dolman, A., van der Molen, M., R. Luning, A. A., Delpierre, N., Gash, J., Lindorth, A., Richardson, A., Verbeeck, H., and Wohlfahrt, G.: Assessing parameter variability in a photosynthesis model within and between plany functional types using global FLUXNET eddy covariance data, Agricultural and Forest Meteorology, 2010.

Jones, G. S., Stott, P. A., and Christidis, N.: Attribution of observed historical near-surface temperature variations to anthropogenic and natural causes using CMIP5 simulations, Journal of Geophysical Research: Atmospheres, 118, 4001–4024, doi:10.1002/jgrd.50239, http://dx.doi.org/10.1002/jgrd.50239, 2013.

Kaminski, T., Knorr, W., Schürmann, G., Scholze, M., Rayner, P. J., Zaehle, S., Blessing, S., Dorigo, W., Gayler, V., Giering, R., Gobron, N., Grant, J. P., Heimann, M., Hooker-Stroud, A., Houweling, S., Kato, T., Kattge, J., Kelley, D., Kemp, S., Koffi, E. N., Köstler, C., Mathieu, P.-P., Pinty, B., Reick, C. H., Rödenbeck, C., Schnur, R., Scipal, K., Sebald, C., Stacke, T., van Scheltinga, A. T., Vossbeck, M., Widmann, H., and Ziehn, T.: The BETHY/JSBACH Carbon Cycle Data Assimilation System: experiences and challenges, Journal of Geophysical Research: Biogeosciences, 118, 1414–1426, doi:10.1002/jgrg.20118, http://dx.doi.org/10.1002/jgrg.20118, 2013.

Knorr, W. and Kattge, J.: Inversion of terrestrial ecosystem model parameter values against eddy covariance measurements by Monte Carlo sampling, Global Change Biology, 11, 1333–1351, 2005.

Kuppel, S., Peylin, P., F.Chevallier, Bacour, C., Maignan, F., and Richardson, A.: Constraining a global ecosystem model with multi-site eddy covariance data, Biogeosciences, 2012.

Kuppel, S., Peylin, P., Maignan, F., F.Chevallier, Kiely, G., Montagnani, L., and Cescatti, A.: Mode-data fusion across ecosystems: from multi-site optimizations to global simulations, Geosci. Model Dev. Discuss., 7, 2961–3011, 2014.

Medvigy, D. and Moorcroft, P. R.: Predicting ecosystem dynamics at regional scales: an evaluation of a terrestrial biosphere model for the forests of northeastern North America, Philosophical Transactions of the Royal Society of London B: Biological Sciences, 367, 222–235, doi:10.1098/rstb.2011.0253, 2011.

Medvigy, D., Wofsy, S. C., Munger, J. W., Hollinger, D. Y., and Moorcroft, P. R.: Mechanistic scaling of ecosystem function and dynamics in space and time: Ecosystem Demography model version 2, Journal of Geophysical Research: Biogeosciences, 114, n/a–n/a, doi:10.1029/2008JG000812, http://dx.doi.org/10.1029/2008JG000812, g01002, 2009.

Papale, D., Reichstein, M., Aubinet, M., Canfora, E., Bernhofer, C., Kutsch, W., Longdoz, B., Rambal, S., Valentini, R., Vesala, T., et al.: Towards a standardized processing of Net Ecosystem Exchange measured with eddy covariance technique: algorithms and uncertainty estimation, Biogeosciences, 3, 571–583, 2006.

Peng, C., Guilot, J., Wu, H., Jiang, H., and Luo, Y.: Integrating models with data in ecology and palaeoecology advances towards a model-data fusion approach, Ecology Letters, 14, 522–536, 2011.

Geosci. Model Dev. Discuss., doi:10.5194/gmd-2015-281, 2016
Manuscript under review for journal Geosci. Model Dev.
Published: 20 January 2016

Pitman, A.: The evolution of, and revolution in, land surface schemes designed for climate models, International Journal of Climatology, 23, 479–510, 2003.

R Development Core Team: R: A Language and Environment for Statistical Computing, R Foundation for Statistical Computing, Vienna, Austria, ISBN 3-900051-07-0, 2015.

Raupach, M., Rayner, P., Barrett, D., Defries, R., Heimann, M., Ojima, D., Quegan, S., and Schmullius, C.: Model-data synthesis in terrestrial carbon observation methods, data requirements and data uncertainty specifications, Global Change Biology, 11, 378–297, 2005.

Rayner, P., Scholze, M., Knorr, W., Kaminski, T., Giering, R., and Widmann, H.: Two decades of terrestrial carbon fluxes from a carbon cycle data assimilation system (CCDAS), Global Biogeochem. Cycles, 19, 2005.

Reichstein, M., Tenhunen, J., Roupsard, O., Ourcival, J.-M., Rambal, S., Miglietta, F., Peressotti, A., Pecchiari, M., Tirone, G., and Valentini, R.: Inverse modeling of seasonal drought effects on canopy CO2/H2O exchange in three Mediterranean ecosystems, Journal of Geophysical Research: Atmospheres (1984–2012), 108, 2003.

Reichstein, M., Falge, E., Baldocchi, D., Papale, D., Aubinet, M., Berbigier, P., Bernhofer, C., Buchmann, N., Gilmanov, T., Granier, A., et al.: On the separation of net ecosystem exchange into assimilation and ecosystem respiration: review and improved algorithm, Global Change Biology, 11, 1424–1439, 2005.

Santaren, D., Peylin, P., Viovy, N., and Ciais, P.: Optimizing a process-based ecosystem model with eddy-covariance flux measurements: A pine forest in southern France, Global biochemical cycles, 21, 2007.

Sellers, P., Dickinson, R., Randall, D., Betts, A., Hall, F., Berry, J., Collatz, G., Denning, A., Mooney, H., Nobre, C., et al.: Modeling the exchanges of energy, water, and carbon between continents and the atmosphere, Science, 275, 502, 1997.

Stocker, T., Qin, D., Plattner, G.-K., Tignor, M., Allen, S., Boschung, J., Nauels, A., Xia, Y., Bex, V., and Midgley, P., eds.: Summary for Policymakers, book section SPM, p. 1–30, Cambridge University Press, Cambridge, United Kingdom and New York, NY, USA, doi:10.1017/CBO9781107415324.004, www.climatechange2013.org, 2013.

Thornton, P. E., Lamarque, J.-F., Rosenbloom, N. A., and Mahowald, N. M.: Influence of carbon-nitrogen cycle coupling on land model response to CO2 fertilization and climate variability, Global Biogeochemical Cycles, 21, n/a–n/a, doi:10.1029/2006GB002868, http://dx.doi.org/10.1029/2006GB002868, gB4018, 2007.

Thum, T., Aalto, T., Laurila, T., Aurela, M., Lindroth, A., and Vesala, T.: Assessing seasonality of biochemical CO 2 exchange model parameters from micrometeorological flux observations at boreal coniferous forest, Biogeosciences, 5, 1625–1639, 2008.

Verbeeck, H., Peylin, P., Bacour, C., Bonal, D., Steppe, K., and Ciais, P.: Seasonal patterns of CO2 fluxes in Amazon forests: Fusion of eddy covariance data and the ORCHIDEE model, Journal of Geophysical Research, 116, 2011.

Wang, Y.-P., Leuning, R., Cleugh, H. A., and Coppin, P. A.: Parameter estimation in surface exchange models using nonlinear inversion: how many parameters can we estimate and which measurements are most useful?, Global Change Biology, 7, 495–510, 2001.

Wang, Y. P., Baldocchi, D., Leuning, R., Falge, E., and Vesala, T.: Estimating parameters in a land-surface model by applying nonlinear inversion to eddy covariance flux measurements from eight Fluxnet sites, Global Change Biology, 13, 652–670, 2007.

Williams, M., Richardson, A., Reichstein, M., Stoy, P., Peylin, P., Verbeeck, H., Carvalhais, N., Jung, M., Hollinger, D., Kattge, J., Leuning, R., Luo, Y., Tomelleri, E., Trudinger, C., and Wang, Y.-P.: Improving land surface models with FLUXNET data, Biogeosciences, 2009.

Xiao, J., Davis, K. J., Urban, N. M., Keller, K., and Saliendra, N. Z.: Upscaling Carbon Fluxes from Towers to the Regional Scale: Influence of Parameter Variability and Land Cover Representation on Regional Flux Estomates, Journal of Geophysical Research, 2011.

Zaehle, S., Friedlingstein, P., and Friend, A. D.: Terrestrial nitrogen feedbacks may accelerate future climate change, Geophysical Research Letters, 37, n/a–n/a, doi:10.1029/2009GL041345, http://dx.doi.org/10.1029/2009GL041345, l01401, 2010.

Geosci. Model Dev. Discuss., doi:10.5194/gmd-2015-281, 2016
Manuscript under review for journal Geosci. Model Dev.
Published: 20 January 2016

Geoscientific Model Development Discussions
Open Access
EGU

Table 1. Parameters in optimisation vector, with descriptions.

Symbol	Name in code	Description	Units
n_0	`nl0`	Top leaf nitrogen concentration	kg N (kg C)$^{-1}$
f_0	`f0`	Maximum ratio of internal to external CO_2	-
d_r	`rootd_ft`	Root depth	m
α	`alpha`	Quantum efficiency	mol CO_2 per mol PAR photons
$\frac{\delta c}{\delta l}$	`dcatch_dlai`	Rate of change of canopy interception capacity with LAI	kg m^{-2}
T_{low}	`tlow`	Lower temperature for photosynthesis	°C
T_{upp}	`tupp`	Upper temperature for photosynthesis	°C
dq_c	`dqcrit`	Humidity deficit at which stomata close	kgkg^{-}1

Geosci. Model Dev. Discuss., doi:10.5194/gmd-2015-281, 2016
Manuscript under review for journal Geosci. Model Dev.
Published: 20 January 2016

Geoscientific Model Development Discussions
Open Access
EGU

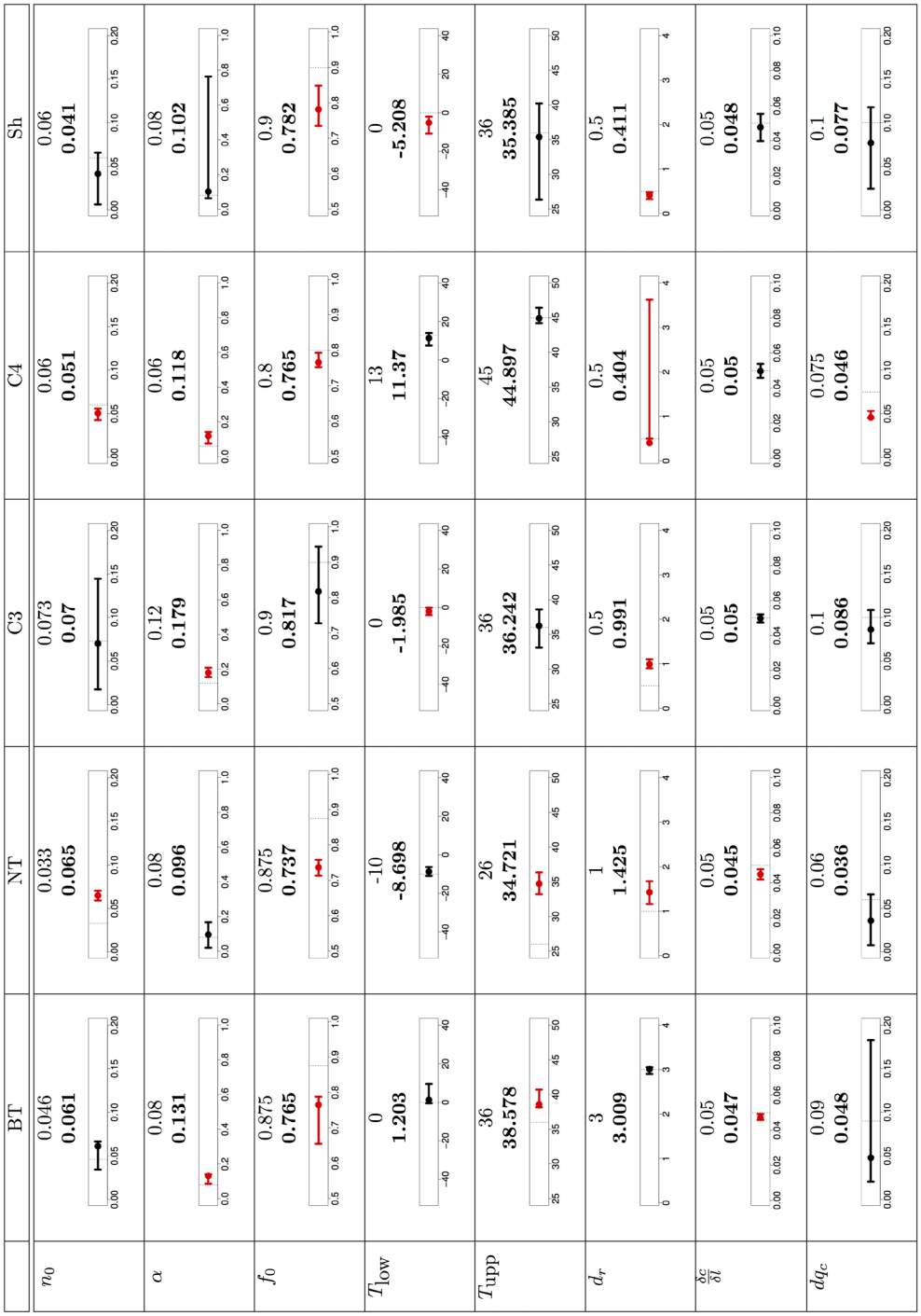

Figure 4. JULES parameters optimised in this study (Table 1). Initial values for each PFT are given, and below in bold are optimised values. The error bars show the uncertainty ranges given as a 80% confidence interval. The range of the box is the allowed range of the parameters were allowed to vary over. Highlighted in red are the error bars for which the prior values (dotted line) are found outside the new uncertainty bounds. A numerical version of this table exists in Appendix B.

Geosci. Model Dev. Discuss., doi:10.5194/gmd-2015-281, 2016
Manuscript under review for journal Geosci. Model Dev.
Published: 20 January 2016

Geoscientific Model Development Discussions

Figure 5. The correlations between the optimised parameters found at each of the PFTs. Each subfigure shows a two-dimensional correlation map and with each subfigure, each box is a 2-D marginal plot. Bar graphs show 1-D marginal distributions of the individual parameters. The dimensions of the boxes represent the allowed range of each parameter. Red points/dashed lines represent initial parameter values. Blue points/dashed lines represent the new optimised parameter values and the blue contours define the cloud of possible parameter values.

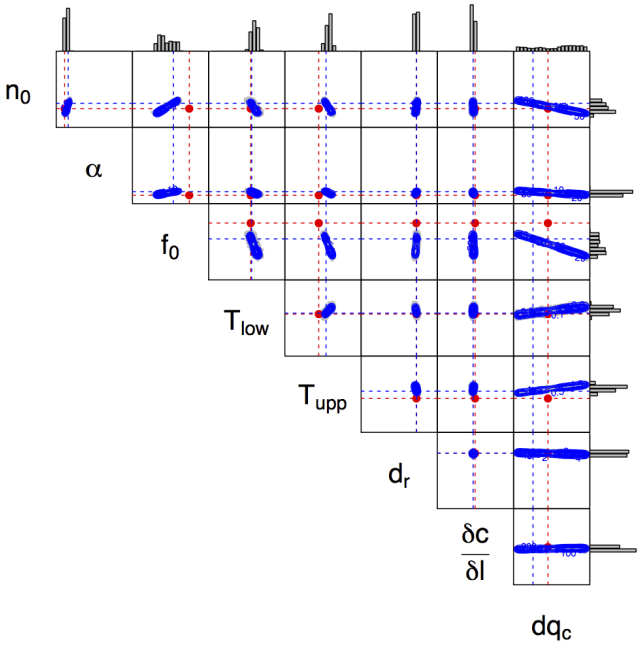

(a) Broadleaf

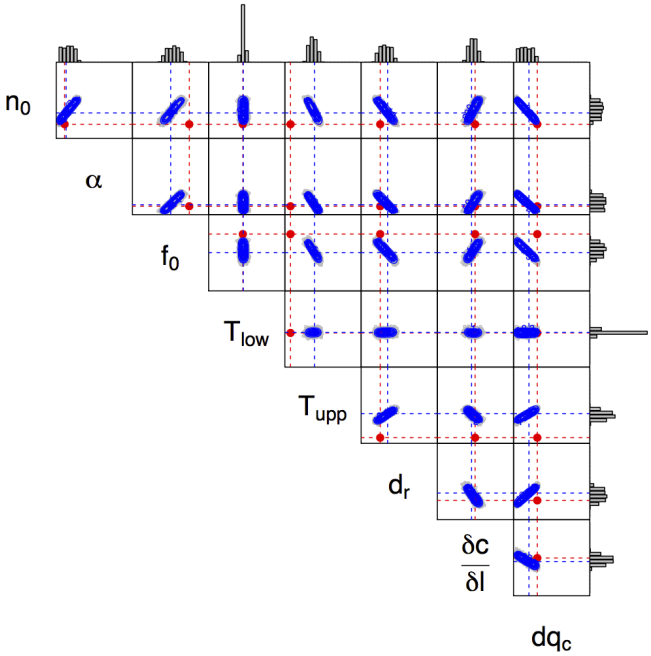

(b) Needleleaf

Geosci. Model Dev. Discuss., doi:10.5194/gmd-2015-281, 2016
Manuscript under review for journal Geosci. Model Dev.
Published: 20 January 2016

Geoscientific Model Development Discussions
Open Access
EGU

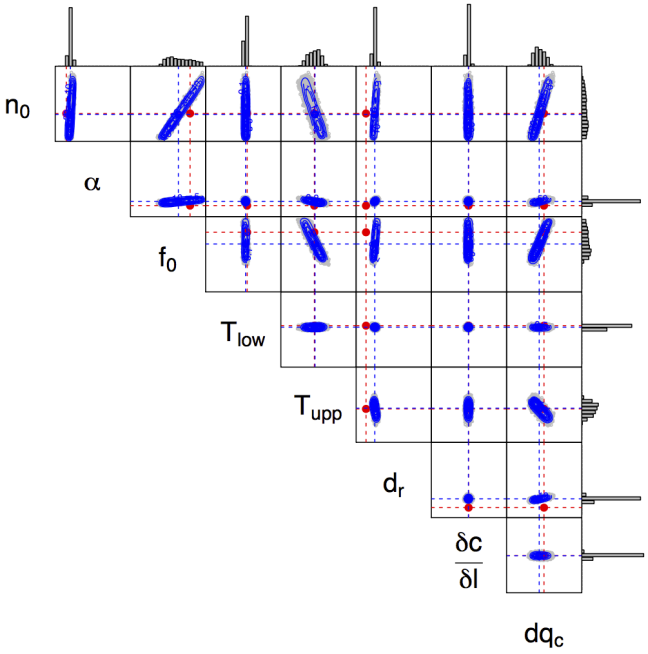

(c) C3 grasses

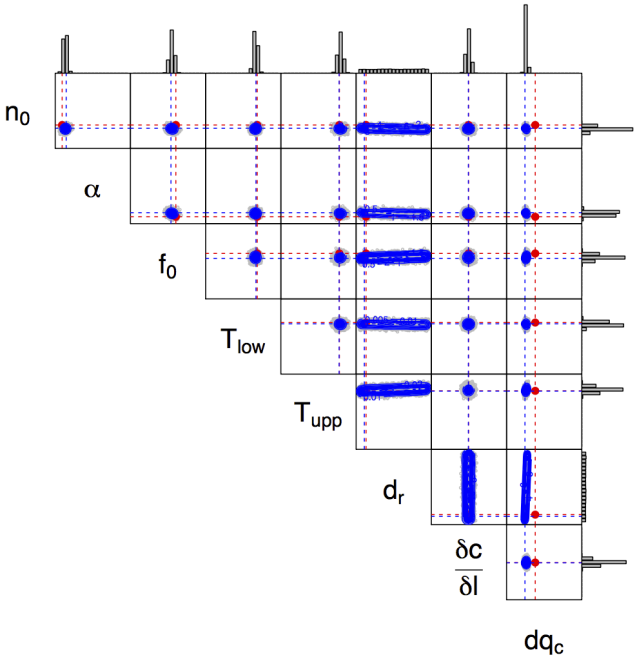

(d) C4 grasses

Figure 5. continued

Geosci. Model Dev. Discuss., doi:10.5194/gmd-2015-281, 2016
Manuscript under review for journal Geosci. Model Dev.
Published: 20 January 2016

Geoscientific Model Development Discussions
Open Access
EGU

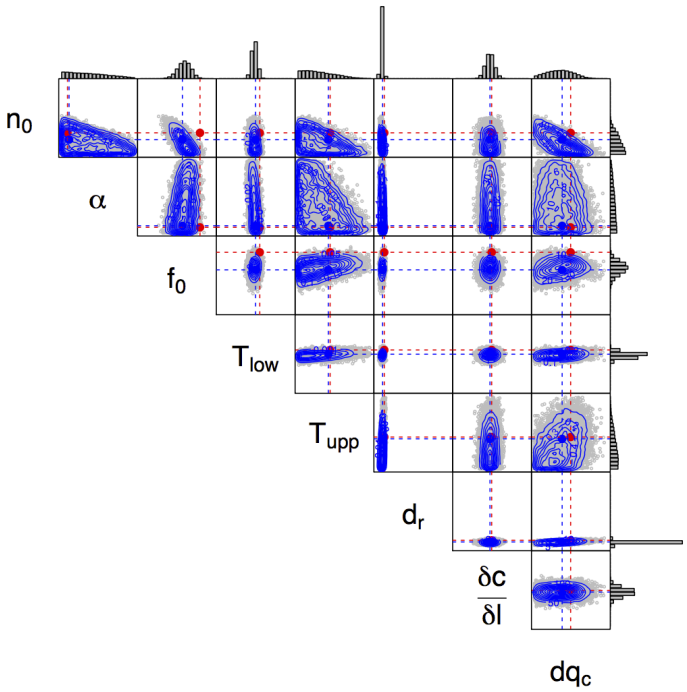

(e) Shrubs

Figure 5. continued

Geosci. Model Dev. Discuss., doi:10.5194/gmd-2015-281, 2016
Manuscript under review for journal Geosci. Model Dev.
Published: 20 January 2016

Geoscientific Model Development Discussions

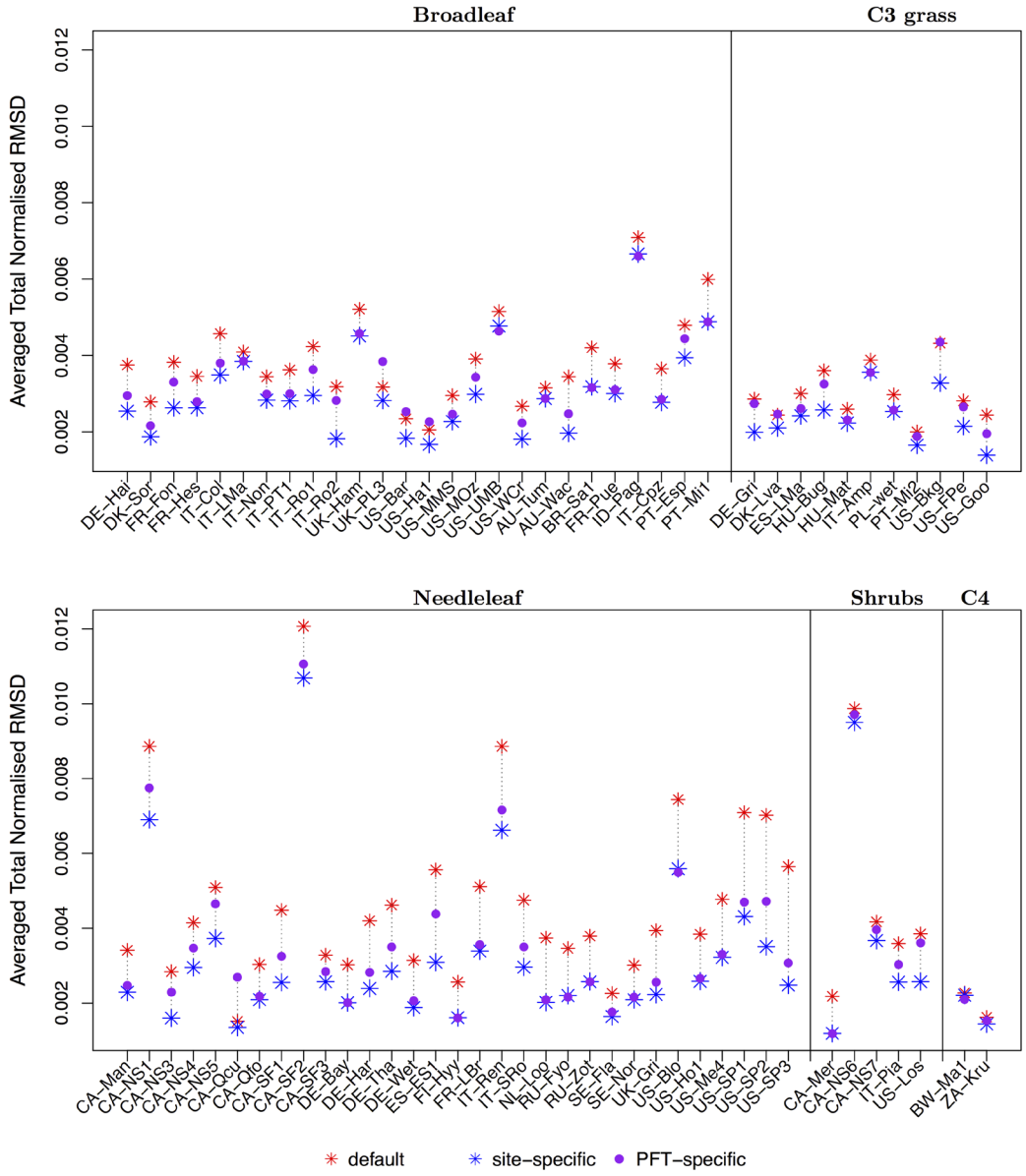

Figure 6. The effect of different parameter vectors on the overall model-data fit at each of the site tested, using the metric described in section 2.5.2. The three z vectors tested: the original default JULES parameters (∗), the parameter vector found by optimising at the individual sites (∗), the new PFT-specific parameter vector found by optimising over the given PFT (•). Outliers with very large initial errors have been removed from the plot shown (Broadleaf: BR-Sa3, IT-Lec, Needleleaf: CA-NS2, SE-Sk2, IT-Yat, IT-Lav).

Geosci. Model Dev. Discuss., doi:10.5194/gmd-2015-281, 2016
Manuscript under review for journal Geosci. Model Dev.
Published: 20 January 2016

Geoscientific Model Development Discussions
Open Access
EGU

Table A1. Sites used in this study, the name code is made from the country (first two letters) and site name (last three letters). The period corresponds to the available years of data for each of the sites.

Site	Period	Experiment Year	Latitude	Longitude
Broadleaf sites (BT)				
DE-Hai	(2000, 2006)	2005	51.0793	10.452
DK-Sor	(1996, 2006)	2006	55.4869	11.6458
FR-Fon	(2005, 2006)	2006	48.4763	2.78015
FR-Hes	(1997, 2006)	2003	48.6742	7.06462
IT-Col	(1996, 2006)	2005	41.8494	13.5881
IT-LMa	(2003, 2006)	2006	45.5813	7.15463
IT-Non	(2001, 2006)	2002	44.6898	11.0887
IT-PT1	(2002, 2004)	2003	45.2009	9.06104
IT-Ro1	(2000, 2006)	2006	42.4081	11.93
IT-Ro2	(2002, 2006)	2004	42.3903	11.9209
UK-Ham	(2004, 2005)	2005	51.1208	-0.86083
UK-PL3	(2005, 2006)	2006	51.45	-1.26667
US-Bar	(2004, 2005)	2005	44.0646	-71.28808
US-Ha1	(1991, 2006)	1996	42.5378	-72.1715
US-MMS	(1999, 2005)	2002	39.3231	-86.4131
US-MOz	(2004, 2006)	2006	38.7441	-92.2
US-UMB	(1999, 2003)	2003	45.5598	-84.7138
US-WCr	(1999, 2006)	2005	45.8059	-90.0799
AU-Tum	(2001, 2006)	2003	-35.6557	148.152
AU-Wac	(2005, 2007)	2006	-37.429	145.187
BR-Sa1	(2002, 2004)	2003	-2.85667	-54.9589
BR-Sa3	(2000, 2003)	2002	-3.01803	-54.9714
FR-Pue	(2000, 2006)	2006	43.7414	3.59583
ID-Pag	(2002, 2003)	2003	2.345	114.036
IT-Cpz	(1997, 2006)	2004	41.7052	12.3761
IT-Lec	(2005, 2006)	2006	43.3046	11.2706
PT-Esp	(2002, 2004)	2004	38.6394	-8.6018
PT-Mi1	(2003, 2005)	2005	38.5407	-8.0004
C3 grasses sites (C3G)				
DE-Gri	(2005, 2006)	2006	50.9495	13.5125
DK-Lva	(2005, 2006)	2006	55.6833	12.0833
ES-LMa	(2004, 2006)	2006	39.9415	-5.77336
HU-Bug	(2002, 2006)	2006	46.6911	19.6013
HU-Mat	(2004, 2006)	2006	47.8469	19.726
IT-Amp	(2002, 2006)	2006	41.9041	13.6052
PL-wet	(2004, 2005)	2005	52.7622	16.3094
PT-Mi2	(2004, 2006)	2006	38.4765	-8.02455
US-Bkg	(2004, 2006)	2006	44.3453	-96.8362
US-FPe	(2000, 2006)	2002	48.3079	-105.101
US-Goo	(2002, 2006)	2006	34.25	-89.97

Geosci. Model Dev. Discuss., doi:10.5194/gmd-2015-281, 2016
Manuscript under review for journal Geosci. Model Dev.
Published: 20 January 2016

Geoscientific Model Development Discussions
Open Access
EGU

Table A1. continued

Site	Period	Experiment Year	Latitude	Longitude
Needleleaf sites (NT)				
CA-Man	(1997, 2003)	2001	55.8796	-98.4808
CA-NS1	(2002, 2005)	2004	55.8792	-98.4839
CA-NS2	(2001, 2005)	2002	55.9058	-98.5247
CA-NS3	(2001, 2005)	2004	55.9117	-98.3822
CA-NS4	(2002, 2004)	2004	55.9117	-98.3822
CA-NS5	(2001, 2005)	2004	55.8631	-98.485
CA-Qcu	(2001, 2006)	2005	49.2671	-74.0365
CA-Qfo	(2003, 2006)	2006	49.6925	-74.3421
CA-SF1	(2003, 2005)	2004	54.485	-105.818
CA-SF2	(2003, 2005)	2004	54.2539	-105.878
CA-SF3	(2003, 2005)	2005	54.0916	-106.005
DE-Bay	(1996, 1999)	1999	50.1419	11.8669
DE-Har	(2005, 2006)	2006	47.9344	7.601
DE-Tha	(1996, 2006)	2005	50.9636	13.5669
DE-Wet	(2002, 2006)	2006	50.4535	11.4575
ES-ES1	(1999, 2006)	2005	39.346	-0.31881
FI-Hyy	(1996, 2006)	2006	61.8474	24.2948
FR-LBr	(2003, 2006)	2006	44.7171	-0.7693
IL-Yat	(2001, 2006)	2005	31.345	35.0515
IT-Lav	(2000, 2002)	2001	45.9553	11.2812
IT-Ren	(1999, 2006)	2005	46.5878	11.4347
IT-SRo	(1999, 2006)	2006	43.72786	10.28444
NL-Loo	(1996, 2006)	2006	52.1679	5.74396
RU-Fyo	(1998, 2006)	2005	56.46167	32.92389
RU-Zot	(2002, 2004)	2003	60.8008	89.3508
SE-Fla	(1996, 1998)	1998	64.1128	19.4569
SE-Nor	(1996, 1999)	1997	60.086	17.480
SE-Sk2	(2004, 2005)	2005	60.12967	17.84006
UK-Gri	(1997, 1998)	1998	56.60722	-3.79806
US-Blo	(1997, 2006)	2006	38.8952	-120.633
US-Ho1	(1996, 2004)	2004	45.2041	-68.7403
US-Me4	(1996, 2000)	2000	44.4992	-121.622
US-SP1	(2000, 2001)	2001	29.7381	-82.2188
US-SP2	(1998, 2004)	2001	29.7648	-82.2448
US-SP3	(1999, 2004)	2001	29.7548	-82.1633
Shrubs sites (Sh)				
CA-Mer	(1998, 2005)	2004	45.4094	-75.5186
CA-NS6	(2001, 2005)	2003	55.9167	-98.9644
CA-NS7	(2002, 2005)	2003	56.6358	-99.9483
IT-Pia	(2002, 2005)	2003	42.5839	10.0784
US-Los	(2001, 2005)	2005	46.0827	-89.9792
C4 grasses sites (C4G)				
BW-Ma1	(1999, 2001)	2000	-19.9155	23.5605
ZA-Kru	(2001, 2003)	2002	-25.0197	31.4969

Geosci. Model Dev. Discuss., doi:10.5194/gmd-2015-281, 2016
Manuscript under review for journal Geosci. Model Dev.
Published: 20 January 2016

Geoscientific Model Development Discussions
Open Access
EGU

Table B1. Parameters of JULES optimised in this study as described in table 1. The prior values for each PFT are given along with the initial ranges allowed. Below in bold are the optimised values and uncertainty ranges given as a 80% confidence interval (in parentheses). Optimised values for which the prior values are found outside the new uncertainty range highlighted by (*).

	BT	NT	C3	C4	Sh
n_0	0.046	0.033	0.073	0.06	0.06
	(0.001,0.2)	(0.001,0.2)	(0.001,0.2)	(0.001,0.2)	(0.001,0.2)
	0.061	**0.065***	**0.07**	**0.051***	**0.041**
	(0.034,0.066)	**(0.059,0.07)**	**(0.018,0.145)**	**(0.043,0.056)**	**(0.006,0.066)**
α	0.08	0.08	0.12	0.06	0.08
	(0.001,0.999)	(0.001,0.999)	(0.001,0.999)	(0.001,0.999)	(0.001,0.999)
	0.131*	**0.096**	**0.179***	**0.118***	**0.102**
	(0.087,0.14)	**(0.021,0.167)**	**(0.155,0.209)**	**(0.075,0.141)**	**(0.063,0.763)**
f_0	0.875	0.875	0.9	0.8	0.9
	(0.5,0.99)	(0.5,0.99)	(0.5,0.99)	(0.5,0.99)	(0.5,0.99)
	0.765*	**0.737***	**0.817**	**0.765***	**0.782***
	(0.655,0.787)	**(0.713,0.758)**	**(0.727,0.944)**	**(0.752,0.793)**	**(0.735,0.848)**
T_{low}	0	-10	0	13	0
	(-50,40)	(-50,40)	(-50,40)	(-50,40)	(-50,40)
	1.203	**-8.698**	**-1.985***	**11.37**	**-5.208***
	(-0.555,9.492)	**(-10.98,-6.342)**	**(-3.877,-0.13)**	**(7.522,14.072)**	**(-10.855,-2.106)**
T_{upp}	36	26	36	45	36
	(25,50)	(25,50)	(25,50)	(25,50)	(25,50)
	38.578*	**34.721***	**36.242**	**44.897**	**35.385**
	(38.157,40.698)	**(33.214,36.365)**	**(33.087,38.599)**	**(44.201,46.426)**	**(26.339,40.216)**
d_r	3	1	0.5	0.5	0.5
	(0.1,4)	(0.1,4)	(0.1,4)	(0.1,4)	(0.1,4)
	3.009	**1.425***	**0.991***	**0.404***	**0.411***
	(2.901,3.052)	**(1.159,1.672)**	**(0.901,1.101)**	**(0.5,3.623)**	**(0.324,0.473)**
$\frac{\delta c}{\delta l}$	0.05	0.05	0.05	0.05	0.05
	(0.001,0.1)	(0.001,0.1)	(0.001,0.1)	(0.001,0.1)	(0.001,0.1)
	0.047*	**0.045***	**0.05**	**0.05**	**0.048**
	(0.046,0.049)	**(0.042,0.048)**	**(0.047,0.052)**	**(0.046,0.054)**	**(0.04,0.055)**
dq_c	0.09	0.06	0.1	0.075	0.1
	(0.001,0.2)	(0.001,0.2)	(0.001,0.2)	(0.001,0.2)	(0.001,0.2)
	0.048	**0.036**	**0.086**	**0.046***	**0.077**
	(0.02,0.183)	**(0.008,0.066)**	**(0.07,0.109)**	**(0.045,0.053)**	**(0.024,0.118)**